Improvement of the Upper Detection Limit of Ionophore-Based H^+-Selective Electrodes: Explanation and Elimination of Apparently Super-Nernstian Responses

Madeline L. Honig,[†] Ariki Haba,[†] Katie M. F. O'Leary,[†] Emily E. A. Robinson, Kuzivakwashe V. Madungwe, Ye Lin,[‡] Chad McGuire,[‡] and Philippe Bühlmann[†,*]

[†] Department of Chemistry, University of Minnesota, (207 Pleasant St. SE, Minneapolis MN 55455, USA

[‡] Emerson Automation Solutions, 6021 Innovation Boulevard, Shakopee, MN 55379, USA

[*] Corresponding author E-mail: buhlmann@umn.edu

Abstract: The response range of an ion-selective electrode (ISE) has been described by counter ion interference at the lower and Donnan failure at the upper detection limit. This approach fails when the potentiometric response at the upper detection limit exhibits an apparently super-Nernstian response, as it has been reported repeatedly for H^+-selective electrodes. While also observed when samples contain other anions, super-Nernstian responses at low pH are a problem in particular for samples that contain phthalate, a common component of commercial pH calibration solutions. This work shows that co-extraction of H^+ and a sample anion into the sensing membrane alone does not explain these super-Nernstian responses, even when membrane-internal diffusion potentials are taken into account. Instead, these super-Nernstian responses are explained by formation of complexes between that anion and at least two protonated ionophore molecules. As demonstrated by experiment and explained with quantitative phase boundary models, the apparently super-Nernstian responses at low pH can be eliminated by restricting the molecular ratio of ionophore and ionic sites. Notably, this conclusion results in recommendations for the optimization of sensing membranes that, in some instances, will conflict with previously reported recommendations from ionic site theory for the optimization of the lower detection limit. This mechanistic insight is key to maximize the response range of these ionophore-based ISEs.

INTRODUCTION

For medical uses of ion-selective electrodes (ISEs),[1-5] the range of analyte concentrations of interest is typically quite narrow,[6] but for many other applications, concentrations of target ions vary substantially. This is true especially for pH sensors,[7-9] which are used widely in healthcare, food sciences, agriculture, environmental monitoring, pollution control, and many manufacturing industries. In such contexts, a wide linear response range is highly desirable, which requires a thorough understanding of the mechanisms that limit lower and upper detection limits. The lower limit of detection is generally determined by interference from ions other than the target ion or by fluxes of target ions through the sensing membrane.[5, 10] Likewise, established theory explains the upper limit of detection as the result of co-extraction of the target ions, along with an ion of opposite charge sign, from the sample into the sensing membrane.[5, 11-13] Because in this process the target ions form complexes with the ionophore, large complex stabilities as well as high concentrations of uncomplexed ionophore in the ISE membrane worsen upper detection limits. Notably, the quantitative description of such co-extraction[14] predicts a gradual decrease of the response slope at the upper detection limit, typically referred to as Donnan failure.[9, 15]

However, a number of reports have been made of ionophore-based H^+-selective electrodes that exhibit near the upper detection limit a response slope that is larger than the expected Nernstian response slope (58.2 mV/decade at 20 ºC). As shown in the following, the observation of such super-Nernstian responses is not limited to particularly unique conditions. They were found for samples that contained various types of anions, ISEs with different membrane matrixes, and ISEs doped with a number of H^+ ionophores and various molar ratios of ionic sites[1,4,5,9,14] and ionophore. They were also observed both for solid-contact ISE[16-20] and ISEs with an inner filling solution.

An early example for such super-Nernstian responses was reported for poly(vinyl chloride) (PVC) membranes plasticized with bis(2-ethylhexyl) sebacate (BEHS), doped with tridodecylamine as ionophore (1% w/w) and potassium tetrakis(*p*-chlorophenyl)borate (KTpClPB) to provide for ionic sites (in a molar ratio of ionic sites and ionophore of 1.0 : 1.6).[21] A super-Nernstian response was observed in the pH range of 4.5 to 3.5 upon addition of HCl to a buffer solution containing borate, phosphate, and citrate. The authors pointed out that while anion interference is expected at low pH, the super-Nernstian response could not be explained. Similarly, microelectrodes with the same ionophore (total concentration 10% w/w), KTpClPB (in a molar ratio of 1.0 : 9.5 to the ionophore), and *o*-nitrophenyl octyl ether (*o*-NPOE) as membrane solvent (no polymeric membrane matrix) exhibited super-Nernstian responses from pH 5.0 to 3.0 (in 0.1 M phosphate buffer).[22-23] Another study with plasticized PVC membranes found super-Nernstian responses at pH 4.5 to 3.5 for ISEs based on several ionophores with an amino group and asserted that the super-Nernstian response could be explained by a general membrane potential equation, which curiously did not comprise terms for the concentrations of the ionic site and ionophore.[24-25] The authors concluded that the super-Nernstian responses can be explained by formation of doubly protonated ionophore molecules, which would require either protonation of their alkyl chains or formation of pentacoordinated nitrogen atoms, both possibilities that are hardly plausible. Very recently, it was shown for two tertiary amino ionophores that the super-Nernstian slope increased with both the ionophore concentration and the ionophore to ionic site ratio, but once again the authors concluded that the reasons for this phenomenon were unclear.[26]

Super-Nernstian responses were also observed in 1 M KCl solutions for fluorous-phase ISEs with perfluoroperhydrophenanthrene as membrane matrix and three fluorophilic trialkylamine ionophores with an ionophore to ionic site ratio of 4:1 or 2:1.[27-29] The pH range of the super-Nernstian responses was pH 2.5 to 5 for the most basic of the three ionophores (i.e., $N[(CH_2)_5(CF_2)_7CF_3]_3$), while for the less basic $N[(CH_2)_4Rf_8]_3$ and $N[(CH_2)_3Rf_8]_3$ the onset of the super-Nernstian response was shifted to pH 2.2 and <2, respectively, suggesting here too that the basicity of the ionophore affects the super-Nernstian response characteristics significantly.

Finally, super-Nernstian responses were reported for polymethacrylate membranes doped with covalently attached trialkylamine ionophores when sample solutions contained phthalate,[30-31] a common component of commercial pH calibration buffers that has been used to calibrate pH glass electrodes for nearly 100 years.[32-34] A shift of the onset of the super-Nernstian response for these polymethacrylate-based electrodes from 3.8 to 5.5 was observed when switching from samples containing only chloride and phosphate as anions to samples containing phthalate, again consistent with co-extraction enhanced by less hydrophilic anions.[30]

In this work, it is shown that these types of super-Nernstian responses are the result of the co-extraction of H^+ and a sample anion into the ionophore-doped sensing membranes, in which the anion then binds to the protonated ionophore with a stoichiometry of 1:2 or higher. It is also shown that membrane-internal diffusion potentials can be excluded as a cause for these super-Nernstian response slopes.

EXPERIMENTAL SECTION

Reagents and Materials. Nanographite powder (GS-4827; graphite platelets with a size distribution 0.10 to 10 µm, Brunauer–Emmett–Teller surface area 165 m^2/g) was obtained from Graphite Store (Northbrook, IL, USA).[35]

Electrode Preparation. ISEs with an inner filling solution, plasticized PVC membranes, and a body made of Tygon tubing were prepared in the usual way. Solid-contact

ISEs with polymethacrylate membranes were prepared by photopolymerization, as reported previously.[30, 36]

For further experimental details, see the Supporting Information.

RESULTS AND DISCUSSION

Super-Nernstian responses of ionophore-based H^+ selective electrodes at the upper detection limit can be explained by a number of different scenarios. The common feature is co-extraction of H^+ along with a sample anion into the ion-selective membrane, followed by association of that anion with multiple protonated ionophore molecules. Figure 1 illustrates the arguably simplest case.

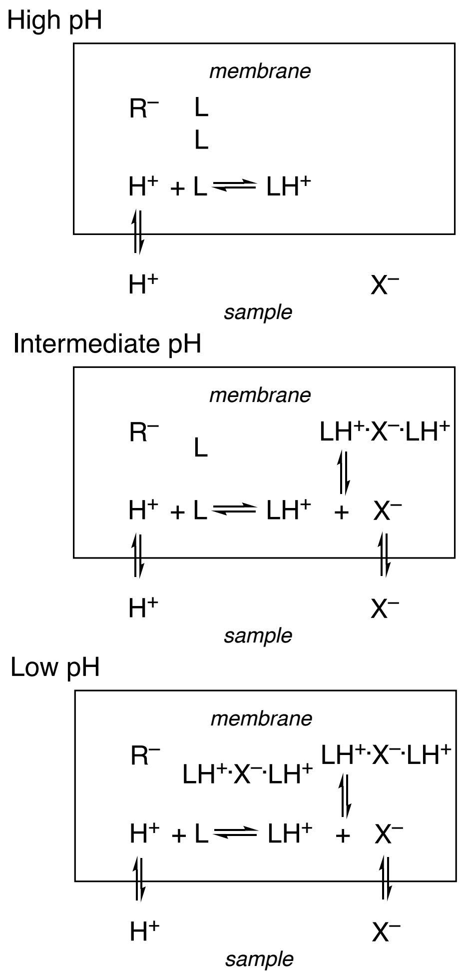

Figure 1. Schematic illustration of the components of an ionophore-doped H^+-selective membrane that exhibits a super-Nernstian response at the upper detection limit (illustrated for a scenario in which the co-extracted anion forms $(LH^+)_2X^-$ complexes with the protonated ionophore).

At a high pH, the sensing membrane contains as the major membrane species besides the anionic sites, R^-, only free ionophore, L, and the protonated ionophore, LH^+. The equilibrium $L + H^+ \rightleftharpoons LH^+$ buffers the activity of the free H^+ in the membrane to a very low and, importantly, constant value, which is required for the ISE to exhibit a Nernstian response to the primary ion H^+.[37] This can be readily understood by considering the phase boundary potential, E_{PB}, at the interface of the sample and the ion-selective membrane,[4, 14] as it can be derived from the electrochemical potentials of H^+ in the two phases:

$$E_{\mathrm{PB}} = E^{\mathrm{o}} + \frac{RT}{F} \ln \frac{a_{\mathrm{H^+}}}{[\mathrm{H^+}]} \quad (1)$$

where $a_{\mathrm{H^+}}$ and $[H^+]$ refer to the activity and concentration of H^+ in the aqueous sample and the sensing membrane, respectively. Assuming that (i) E_{PB} is the only contribution to the measured potential that is sample dependent, (ii) local equilibration is achieved at the interface of the membrane and the sample solution, and (iii) activity coefficients for all ionic species in the membrane are constant and, therefore, concentrations may be used in all equilibrium constants rather than activities,[4, 14] it follows that a linear (Nernstian) dependence of the measured potential on $\ln a_{\mathrm{H^+}}$ is expected for any range of sample pH in which $[H^+]$ in the membrane is constant. [14, 37-38]

In the intermediate pH region (in which the super-Nernstian response is observed; see Figure 2A), co-extraction of an anion, X^-, and H^+, sets in. The H^+ binds to the ionophore, and X^- forms 1:2 complexes with the protonated ionophore, i.e., $(LH^+)_2X^-$. Because only one new LH^+ is formed for every X^- and H^+ entering the membrane while two LH^+ are required to form the complex $(LH^+)_2X^-$, co-extraction stops at a point where the membrane still contains a large amount of free ionophore but all LH^+ is involved in the formation of $(LH^+)_2X^-$ complexes.

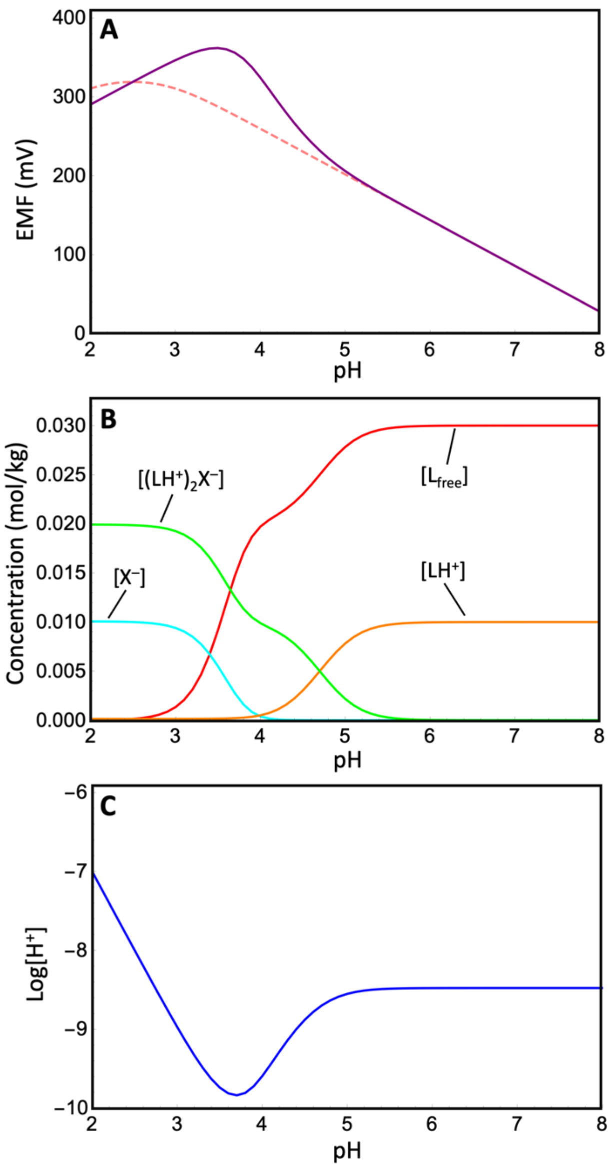

Figure 2. Response of an ionophore-doped H^+-selective membrane that exhibits a super-Nernstian response because of co-extraction of an anion that forms $(LH^+)_2X^-$ complexes in the ISE membrane: (A) Measured potential. (B) Concentrations of major species in the sensing membrane. (C) Log $[\mathrm{H}^+]$ in the sensing membrane. Calculated for $\beta_{\mathrm{LH}} = 10^8$ mol^{-1} kg, $\beta_{(\mathrm{LH})_2\mathrm{X}} = 10^8$ mol^{-2} kg^2, $K_{\mathrm{HXdis}} = 10^{-5}$, $[\mathrm{L_{tot}}] = 4.0\times10^{-2}$ mol kg^{-1}, $[\mathrm{R}^-] = 1.0\times10^{-2}$ mol kg^{-1}, $a_{\mathrm{X}^-} = a_{\mathrm{H}^+}$, and $E^{\mathrm{o}} = 0$ mV.

Only at a very low pH, the concentrations of X^- and H^+ in the sample have become so high that there is no longer a need for the additional boost for the transfer of X^- into the membrane that results from the formation of $(LH^+)_2X^-$. Co-extraction sets in again, leading to the observation of a maximum in the measured potential (see Figure 2A). At the end of this second wave of co-extraction, all the ionophore is protonated. Because there is not enough ionophore in the membrane to bind all X^- in the form of $(LH^+)_2X^-$, some of the anions remain in a free form. Alternatively, they might form ion pairs of the type $(LH^+)X^-$ (see below).

Calculation of the Phase Boundary Potential

Applying the well-established phase boundary model to the system described by Figure 1, computation of the interfacial potential at the boundary of an aqueous sample and the ion-selective membrane by taking into account all relevant chemical equilibria is straightforward. Specifically, the stability of the protonated ionophore is given by:

$$\beta_{\mathrm{LH}} = [\mathrm{LH^+}]/([\mathrm{L}][\mathrm{H^+}]) \tag{2}$$

where [L] and $[LH^+]$ refer to the concentrations of the ionophore and its complex with H^+ in the sensing membrane. The stability of $(LH^+)_2X^-$ is given by:

$$\beta_{(\mathrm{LH})_2\mathrm{X}} = [(\mathrm{LH^+})_2\mathrm{X^-}]/([\mathrm{LH^+}]^2[\mathrm{X^-}]) \tag{3}$$

where $[X^-]$ refers to the anion concentrations in the membrane. The equilibrium constant describing the distribution of H^+ and X^- between the sample and the membrane is defined by:

$$K_{\mathrm{HXdis}} = ([\mathrm{H^+}][\mathrm{X^-}])/(a_{\mathrm{H^+}}\, a_{\mathrm{X^-}}) \tag{4}$$

where $a_{\mathrm{X^-}}$ refers to the activity of the anion in the sample. The mass balance for the ionophore is given by:

$$[\mathrm{L_{tot}}] = [\mathrm{L}] + [\mathrm{LH^+}] + 2\,[(\mathrm{LH^+})_2\mathrm{X^-}] \tag{5}$$

where $[\mathrm{L_{tot}}]$ stands for the total ionophore concentration. Finally, bulk electroneutrality of the membrane requires that:

$$[\mathrm{H^+}] + [\mathrm{LH^+}] + [(\mathrm{LH^+})_2\mathrm{X^-}] = [\mathrm{R^-}] + [\mathrm{X^-}] \tag{6}$$

where $[R^-]$ stands for the concentration of hydrophobic anionic sites that are for practical purposes confined to the membrane phase.

The set of Equations 2 to 6 can be solved to give $[H^+]$ as a function of β_{LH}, $\beta_{(LH)_2X}$, K_{HXdis}, $[L_{tot}]$, $[R^-]$, a_{H^+}, and a_{X^-} (for details, see the Supporting Information). Finally, insertion of the thus obtained expression for $[H^+]$ into Equation 1 describes E_{PB} for the entire pH range as a function of the activities of H^+ and X^- in the sample. Moreover, the expression for $[H^+]$ as a function of β_{LH}, $\beta_{(LH)_2X}$, K_{HXdis}, $[L_{tot}]$, $[R^-]$, a_{H^+}, and a_{X^-} can be used in combination with Equations 2 to 6 to compute the concentration of all species in the sensing membrane as a function of the sample pH and a_{X^-} (for details, see the Supporting Information).

Dependence of the Phase Boundary Potential and Membrane Components on pH

The solid line in Figure 2A shows E_{PB} as a function of the sample pH for a set of representative parameters of β_{LH}, $\beta_{(LH)_2X}$, K_{HXdis}, $[L_{tot}]$, $[R^-]$, and a_{X^-}. At pH > 5, a Nernstian response is observed. This is consistent with a $[H^+]$ that in this pH region is sample-independent (shown in Figure 2C). An apparently super-Nernstian response is observed from pH 5 to 3.7. This is possible because $[H^+]$ in this pH region is *decreasing* with the increasing concentration of a_{H^+}, as predicted by Equation 1 and illustrated by Figure 2C.

Figure 2B illustrates the cause for this decrease in $[H^+]$ in the membrane while a_{H^+} is increasing. The co-extraction of H^+ and X^- into the sensing membrane results in the protonation of ionophore, consistent with a decrease in the free ionophore concentration, [L]. However, this does not result in an increase in the concentration $[LH^+]$. Instead, because every X^- that enters the membrane binds two LH^+, the extraction of X^- into the sensing membrane leads to a decrease in $[LH^+]$. For a sensing membrane in which $[L_{tot}]$ is sufficiently large as compared to $[R^-]$, the relative change in $[LH^+]$ with increasing a_{H^+} is larger than the relative change in

$[\mathrm{L}]$, and, therefore, it follows from Equation 2 that $[\mathrm{H}^+]$ has to decrease. This is confirmed by Figure 2C.

Notably, the slope of E_{PB} steadily increases from about pH 5 to a maximum at around pH 4.2, where most of the LH^+ has been used up to form $(\mathrm{LH}^+)_2\mathrm{X}^-$ but the concentration of free X^- in the membrane is still low. As the pH further decreases, co-extraction H^+ and X^- into the membrane continues and is still assisted by LH^+, but while every H^+ entering the membrane can still bind to an ionophore, only every second X^- can form a $(\mathrm{LH}^+)_2\mathrm{X}^-$ complex. Consequently, $[\mathrm{X}^-]$ starts to increase substantially. The reduced driving force for co-extraction of H^+ and X^- into the membrane is reflected by a gradual decrease in the response slope as the pH falls below 4.2.

By comparison, the dashed line in Figure 2A shows E_{PB} as computed for the same set of parameters as for the solid line, except for $\beta_{(\mathrm{LH})_2\mathrm{X}}$, which is given such a low value that $(\mathrm{LH}^+)_2\mathrm{X}^-$ is not being formed. In this case, the response remains Nernstian until co-extraction of H^+ and X^- into the membrane causes the slope to gradually decrease.

Alternative Stoichiometries That Cause Super-Nernstian Responses

A number of scenarios similar to the one shown in Figure 1 are predicted to cause super-Nernstian responses very similar to the one illustrated with Figure 2. This includes variations of the set of equilibria represented by Figure 1 in which X^- and LH^+ do not form aggregates with a 1:2 stoichiometry but, instead, 1:3, 1:4, or higher. Moreover, the stoichiometry of the complexes of X^- and LH^+ does not have to be exclusive; e.g., $(\mathrm{LH}^+)_2\mathrm{X}^-$ and $(\mathrm{LH}^+)\mathrm{X}^-$ may be formed simultaneously. In yet another variation, aggregates of the type $(\mathrm{LH}^+)_n\mathrm{X}^-$ may form a hydrogen bond to a free ionophore, resulting in the formation of $(\mathrm{LH}^+)_n\mathrm{X}^-(\mathrm{L})$. This appears likely for an anion with a hydrogen bond donor group, such as hydrogen phthalate. Also, any of these species could further form additional ion pairs and higher ion aggregates. Importantly, all these scenarios share the common feature that X^- forms at least one aggregate that comprises more than one LH^+. On the other hand, several alternative sets of equilibria that did not include formation of an aggregate of X^- with more than one LH^+ failed to explain super-Nernstian slopes. This included equilibria that involved the formation of species such as HX, $XH{\bullet}X^-$, $LH^+{\bullet}X^-$, $LH^+{\bullet}X^-{\bullet}HX$, or $LH^+{\bullet}X^-{\bullet}L$.

Determining which of these scenarios explains the super-Nernstian response of a particular ISE will in most cases be less important than finding a way to eliminate the super-Nernstian response and, thereby, widen the linear response range. This is possible by modifying the composition of the sensing membrane, as shown in the following.

Dependence of the Super-Nernstian Response on the Molecular Ratio of Ionophore and Ionic Sites

Figure 3 shows E_{PB} as a function of pH as computed for a range of values of $[\mathrm{L_{tot}}]$ and the same values of β_{LH}, $\beta_{(\mathrm{LH})_2\mathrm{X}}$, K_{HXdis}, and $[\mathrm{R}^-]$ as for the solid line in Figure 2. The optimum upper detection limit is achieved for molar ratios of the ionophore and ionic site of 2. For larger ratios, the onset of the super-Nernstian response range shifts continuously to higher pH values. And for molar ratios of the ionophore and ionic site smaller than 2, the response slope gradually decreases with decreasing pH as is commonly observed for Donnan failure, and the onset of this slope decrease shifts to higher pH the smaller the ionophore-to-ionic site ratio. Notably, for the ionophore-to-ionic site ratio of 2 and an anion that precipitates as HX in the sample at pH ≤ 3 (as this is the case for phthalic acid), E_{PB} varies linearly with pH in the entire pH range (see Figure S5).

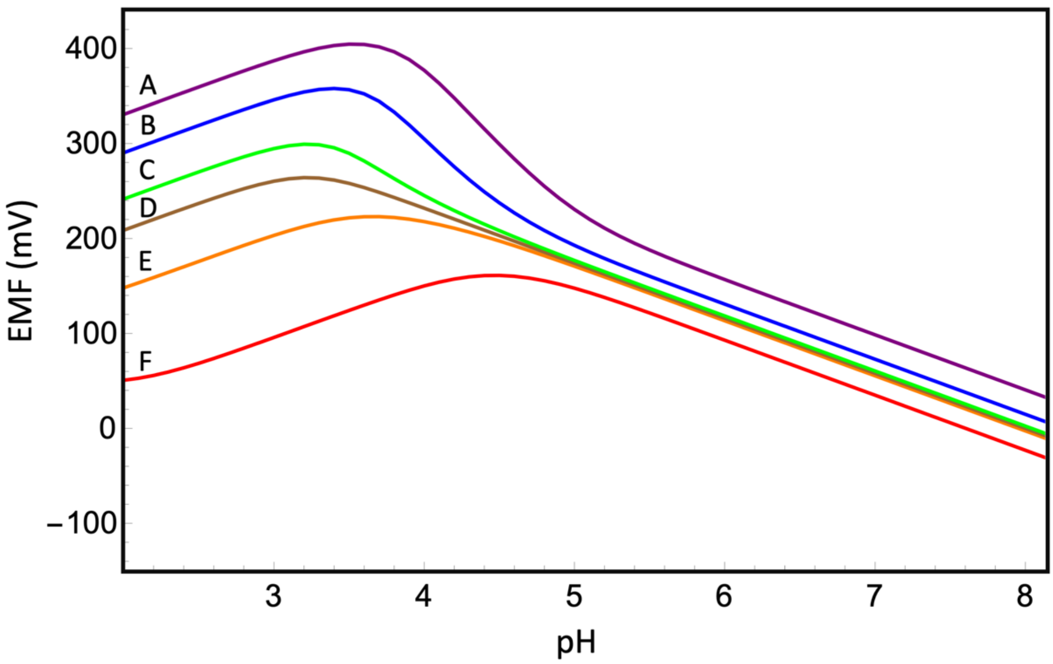

Figure 3. Response of ionophore-doped H^+-selective membrane that exhibits a super-Nernstian response because of co-extraction of an anion that forms $(LH^+)_2X^-$ complexes in the ISE membrane, calculated for different values of $[L_{tot}] = 15\times10^{-2}$ (A), 7.0×10^{-2} (B), 5.25×10^{-2} (C), 5.0×10^{-2} (D), 4.75×10^{-2} (E), and 3.5×10^{-2} (F) mol kg^{-1} as well as $\beta_{LH} = 10^8$mol^{-1} kg, $\beta_{(LH)_2X} = 10^8$ mol^{-2} kg^2, $K_{HXdis} = 10^{-5}$, $[R^-] = 2.5\times10^{-2}$ mol kg^{-1}, $a_{X^-} = a_{H^+}$, and $E^o = 0$ mV.

The dependence of E_{PB} on pH as shown in Figure 3 is unique to the set of chemical equilibria as represented by Figure 1. As there are other sets of chemical equilibria that also give rise to super-Nernstian responses at the upper detection limit, and as each of these scenarios is characterized by its own distinctive dependence of E_{PB} on pH and the ionophore-to-ionic site ratio, it is not possible without additional experimental evidence to predict for a particular type of ionophore and sample ion which ionophore-to-ionic site ratio gives the highest upper detection limit. However, Figure 3 clearly illustrates that experimental variation of the ionophore-to-ionic site ratio can be used to improve the upper detection limit.

Experimental Observation of Super-Nernstian Responses in the Presence of Chloride, Phosphate, or Hydrogen Phthalate

Experimental examples for super-Nernstian responses at the upper detection limit are shown in Figure 4 for ISEs with PVC membranes plasticized with *o*-NPOE and doped with the ionophore tridodecylamine and ionic sites (in a 25 mol % with respect to the ionophore). Super-Nernstian responses were observed both for chloride and phosphate as counter ion, but the extent of the deviation from the linear (Nernstian) response depends on the type of the counter ion. This is also evident from Table S1, which highlights that, for identical ISE membranes, the onset of the super-Nernstian response is found for chloride at a more than one unit higher pH than for phosphate. This is indeed expected, given the much larger hydrophilicity of phosphate as compared to chloride.[39]

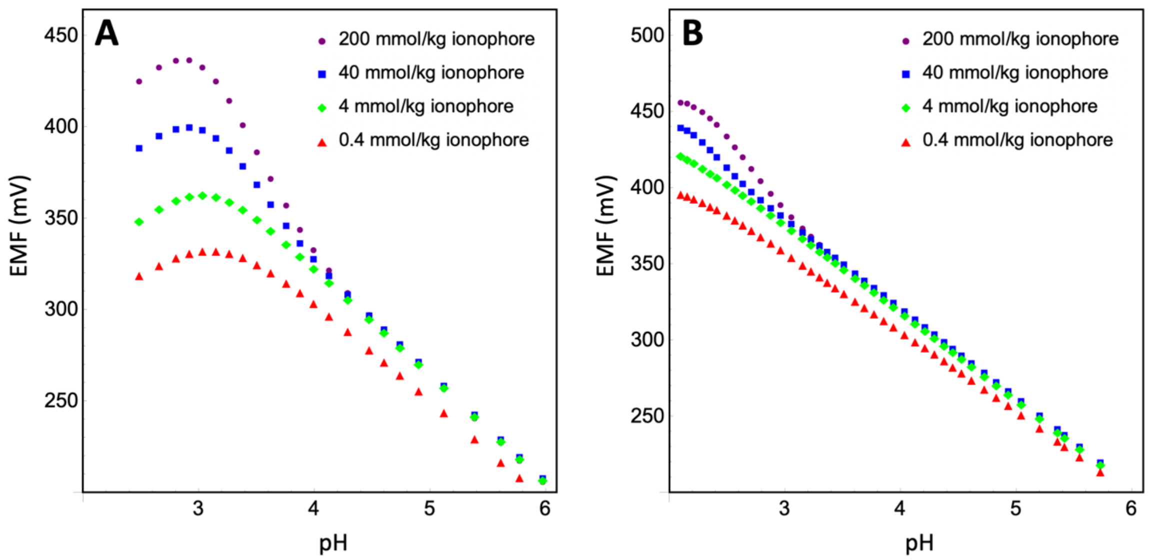

Figure 4. Experimental potential responses of an ISE with a plasticized *o*-NPOE/PVC membrane with tridodecylamine as H^+ ionophore and tetrakis(pentafluorophenyl)borate) as ionic sites (molecular ratio of ionophore to ionic sites 4:1) when immersed in a 1.0 mM borate buffer; pH adjusted by addition of (A) HCl and (B) phosphoric acid.

Note that a quantitative definition for the onset of a super-Nernstian response was required for this work. We chose the logarithm of the target ion activity at which the experimentally measured emf is 5 mV higher than what would be predicted based on a linear extrapolation of the emf from the linear response range. A definition resembling more closely the extrapolation of two linear response regions, as this is recommended by IUPAC for the lower detection limit,[40] was not possible because the super-Nernstian response region of these electrodes does not exhibit a subsection in which the response is changing linearly with the pH (i.e., the slope of the potential versus pH curve is continuously changing).

Also consistent with the theoretical discussion above is the observation that a super-Nernstian response was only observed for the ISE membranes that contained the higher ionophore concentrations (200 and 40 mmol/kg; see Figure 4 and Table S1). This was found to be true both for the pH responses to HCl and to H_3PO_4. For the lower ionophore concentrations, the response gradually decreased with the pH until the measured potential reached a maximum, followed by an anionic response, as this is commonly observed for Donnan failure. The same effect is also illustrated in Figure S1 of the Supporting Information, which shows measured potentials for ISE membranes with a constant ionic site concentration and a variable ionophore concentration.

Notably, as illustrated by Figure 4, if a super-Nernstian response is observed, the nature of the counter anion does not only shift the response curve with respect to pH, but it also affects how much the emf deviates from the extrapolated Nernstian response. Predicting this deviation quantitatively is more complex, as it depends on a number of factors, including $\beta_{\mathrm{(LH)_2X}}$, K_{HXdis}, and, if applicable, $\beta_{\mathrm{(LH)X}}$ or $\beta_{\mathrm{(LH)}_n\mathrm{X(LH)}}$. Moreover, while we can exclude diffusion potentials within the membrane as the primary cause of these super-Nernstian responses (see below), it is quite possible that diffusion potentials caused by the co-extraction of H^+ and the counter ion into the membrane slightly modify the exact shape of the response curve. However, determining numerical values that describe the super-Nernstian response in every detail will typically be less important than having a design principle to eliminate this super-Nernstian response.

A super-Nernstian response is also shown in Figure S2 for PVC membranes plasticized with BEHS and doped with tridodecylamine as ionophore and KTpClPB as ionic sites (46 mol % with respect to the ionophore). This example confirms that super-Nernstian responses are not unique to the use of a particular plasticizer or ionic site. As the data shown in Figure S2 have been obtained with solutions that contained a background of 100 mM phthalate, they also give an example for another counter ion that causes super-Nernstian responses. Ionophore-free ion-exchanger ISEs have a high selectivity for hydrogen phthalate, showing a low hydrophilicity for this anion.[41] Therefore, it is not surprising that, for such a high concentration of phthalate in the samples as 100 mM, onset of the super-Nernstian response was observed at pH 6.26 ± 0.03. Phthalate is not only a practically very relevant interferent as it is found in many commercial pH calibration solutions, but it also allowed us to gain further evidence for the proposed response mechanism of the super-Nernstian response using ^{1}H NMR spectroscopy.

For this purpose, ISE membranes with the same composition as used for Figure S2 were equilibrated fully with 100 mM phthalate solutions of pH 6, 5, 4, and 3.5. (Solutions of lower pH were not prepared because phthalic acid has a solubility limit[42] of 0.0427 mol/kg and precipitates at pH ≤3; see Figure S3 of the Supporting Information.) The membranes were than dissolved in THF-d_8, one of the few NMR solvents that completely dissolves all membrane components, and ^{1}H NMR spectra were used to determine the ratio of hydrogen phthalate and ionic sites (see Table S2). This shows that near the onset of the super-Nernstian response (i.e., pH 6), the membranes already contain a significant amount of phthalate (35 mol % with respect to the ionic sites). At pH 5, which coincides with the maximum in the measured potential, the membranes contain 117 mol % hydrogen phthalate with respect to the ionic sites. This value is within error identical with the 117 mol % free ionophore present in the membranes in the absence of hydrogen phthalate, and it suggests that coextraction of H^+ and hydrogen phthalate results at pH 5 in the protonation of all available ionophore, with hydrogen phthalate as the dominant anion in the ISE membrane. This is consistent with the response mechanism described by Figures 1 and 2, and it agrees with the finding that ionophore-free ion-exchanger ISEs were found to respond only to hydrogen phthalate but not the dianion phthalate.[41] At pH 4 and 3.5, the hydrogen phthalate concentration in the membrane increases further. Because at this point there is no free ionophore left in the membrane, the H^+ coextracted along with hydrogen phthalate into the membrane must be present in the form of fully protonated phthalic acid, solvated H^+ ions, or aggregates between these species and hydrogen phthalate. This no longer fulfills the criteria for a super-Nernstian response and is consistent with the experimentally observed potential maximum at pH 5.

The general nature of the super-Nernstian response mechanism of ionophore-based H^+-selective electrodes is further confirmed by very similar observations for the interference of phthalate on solid-contact ISEs with polymethacrylate-based sensing membranes (Figures S6 and S7). This confirms that super-Nernstian responses of this type are not only observed with plasticized PVC membranes, and that they are not limited to ISEs with an inner filling solution, as it is indeed expected based on the response mechanism proposed above. The super-Nernstian responses are only observed for high ratios of ionophore and ionic sites and for high ionophore concentrations (Figures S6 and S7, Tables S3 and S4), as was also observed for ISEs with plasticized PVC membranes. Most importantly, the data show that reduction of the ionophore concentration improves the upper detection limit by three pH units.

As noted in the introduction, there have been various examples for super-Nernstian responses of ionophore-based H^+-selective electrodes in the literature. None of those studies were performed as systematically as this work, which prevents careful interpretation without further study. However, it is notable that several of these studies used sensing membranes with relatively large ionophore to ionic site ratios,[23, 26-27, 29] consistent with the conclusion here that high ionophore concentrations make the observation of super-Nernstian responses more likely. Also consistent with the explanation provided here is the observation that both more hydrophobic counter ions and more basic ionophores shift the onset of the super-Nernstian response to a higher pH.[24-26, 29-30]

Exclusion of Membrane-Internal Diffusion Potentials as a Cause for Super-Nernstian Responses

The theory and experimental results shown above demonstrate that the super-Nernstian responses of ionophore-based H^+ selective electrodes can be explained by quantitative modeling of the multiple chemical equilibria at the interface of the ISE membrane and samples. While one might consider the occurrence of membrane-internal diffusion potentials as an alternative cause for super-Nernstian responses, there is evidence that makes such an explanation unlikely.

Membrane-internal diffusion potentials are expected when an ISE membrane contains different concentrations or types of ionic components on its side facing the sample and its side facing either the internal solution or a solid contact.[5, 43-44] The literature suggests that such diffusion potentials are a few tens of mV at most.[44] Indeed, in many specific contexts, the effect of diffusion potentials can be considered negligible, such as within the Nernstian response range of an ISE, when an ISE membrane contains a hydrophobic electrolyte such as ETH 500, or when interfering ions form ionophore complexes with the same stoichiometry as the target ions.[5]

In contrast, one can expect a sizeable change in the membrane-internal diffusion potentials at the upper detection limit of an ISE, where co-extraction of target and counter ions into the ISE membrane occurs (typically referred to as Donnan failure), increasing the type and concentration of ionic species in the membrane. An example for this was reported by Kakiuchi and Senda, who observed a maximum in the measured potential for an ionophore-free tetrabutylammonium ion exchanger membrane, followed by a drop of the potential by 23 mV upon further increasing the tetrabutylammonium concentration. Theory predicts that at the upper detection limit the phase boundary potential of an ionophore-free ion-exchanger ISE should flatten out, implying that the observed potential decrease was indeed the manifestation of a diffusion potential. However, we are not aware of an example from the literature in which the response slope was increased by a diffusion potential to a value larger than what is expected for a Nernstian response.

To evaluate whether an increase in the predicted emf could be achieved under very special conditions, we modified our phase boundary model for ionophore-based H^+ selective electrodes by addition of a membrane-internal diffusion potential, modeled using the Henderson equation.[45] We assumed that the ionophore was not involved in the formation of complexes other than LH^+, and that the only species contributing to a diffusion potential are LH^+, R^+, and X^-. Representative results are shown in Figures S8 and S9. Analogous to experimental findings of Kakiuchi and Senda for ionophore-free systems, we found that membrane-internal diffusion potentials are likely to affect the pH at which Donnan failure sets in, with a worsening of the upper detection limits when the mobility of the counter ion in the sensing membrane is larger than the mobilities of the other ions and an improvement of the upper detection limit when the mobility of LH^+ exceeds the mobilities of other ions. Most importantly, even with very extreme differences in the mobilities of all ions involved, a super-Nernstian response could not be predicted (see Figures S8 and S9).

The conclusions from this theoretical discussion are consistent with observations made with plasticized PVC membranes doped with the hydrophobic electrolyte tetradodecylammonium tetrakis(3-chlorophenyl)borate (ETH500-m) in addition to ionophore and ionic sites. While the electrolyte would be expected to reduce or even eliminate a membrane-internal diffusion potential, no effect of ETH500-m on the super-Nernstian response was observed (see Figure S10).

In the case of the ISEs with polymethacrylate sensing membranes for which results are shown in Figures S6 and S7, there is yet another reason that rules out diffusion potentials as an explanation for the observation of super-Nernstian responses. In that case, the ionophore is covalently attached to the polymeric membrane matrix. Consequently, at the upper detection limit, X^- is the only mobile species that increases in concentration in the sensing membrane as a result of co-extraction. Large concentrations of uncomplexed H^+ are only expected at a much lower pH, when all the ionophore has been converted to LH^+. Because the only major species that increases in concentration carries a negative charge, any change in the membrane-internal diffusion potential decreases the response slope of the ISE rather than increasing it, as that is necessary to explain a super-Nernstian response.

Conclusions

Slow kinetics resulting from mass transfer limitations were long misunderstood to be the only cause of super-Nernstian responses of ISEs.[10, 46-51] This changed when apparently "twice-Nernstian" responses were explained by the co-existence in the ISE membrane of complexes of an ionophore with both the target cation and a secondary cation over a wide range of target ion activities in the sample[38] (as also observed recently in the context of ion transfer voltammetry[52]). The generalization of this model predicted apparently "sub-Nernstian" responses if the target and secondary ions that form complexes with the ionophore have charges of opposite sign. However, prior examples for apparently "super-Nernstian" responses involving a sample cation and anion were limited to ionophore-free ion-exchanger electrodes with membranes in which the sample cation and anion form complexes with one another.[53-54] Characteristic for all these systems is that the potentiometric response can be explained based on the chemical equilibria at the sample–membrane interface, without consideration of kinetic effects.[38, 53-58]

This work explains the response mechanism of ionophore-based ISEs with apparently "super-Nernstian" responses that can be explained based on chemical equilibria that involve both sample cations and anions. Such responses have been observed numerous times in the past but were not understood mechanistically. These responses differ from prior examples of "super-Nernstian" responses in two aspects. On one hand, the membrane species that explain these super-Nernstian responses are not complexes of the ionophore with either the anion or the cation. Instead, they are, in the simplest case, complexes of the type $(\mathrm{LH}^+)_2\mathrm{X}^-$ that involve both the cation and anion. Higher aggregates of the type $(\mathrm{LH}^+)_{n>2}\mathrm{X}^-$ as well as mixed complexes of the type $(\mathrm{LH}^+)_{n\geq 2}\mathrm{X}^-(\mathrm{L})_{m\geq 1}$ are conceivable as well. On the other hand, unlike in the case, e.g., of apparently "twice-Nernstian" responses, the super-Nernstian responses at the upper detection limit, as explained here, do not exhibit a range of the activity of the target ion in the sample in which the response slope is independent of the target ion activity in the sample. Instead, the derivative of the response slope in the entire super-Nernstian response region is continuously changing with pH. This might raise the suspicion that membrane-internal diffusion potentials could provide an alternative explanation for these super-Nernstian responses, but quantitative modeling and experimental evidence suggest otherwise.

Understanding this response mechanism will allow the developer of ISEs to design sensing membranes that do not exhibit super-Nernstian responses and, as a result, provide the widest possible ranges of the linear response to pH. This work showed that high upper detection limits can be achieved for ISEs comprising polymethacrylate membranes with covalently attached bis(isopropyl)amino groups as ionophore by keeping the ionophore concentration small. Keeping the molecular ratio of the ionophore and ionic sites small is also beneficial, as long as this ratio is not smaller than unity, at which point the ISEs would lose their H^+ selectivity. Notably, this results in a recommendation opposite to that of ionic site theory as reported previously,[5, 59] which predicts an improvement of the selectivity for the primary ion over interfering ions that do not bind to the ionophore when the molecular ratio of the ionophore and ionic sites is increased.

As shown in this work, super-Nernstian responses at the upper detection limit can be explained by multiple scenarios of aggregation and complex formation in the sensing membrane. We recommend that, whenever an electrode exhibits such a response, both the ionophore concentration and the ratio of ionophore and ionic sites be varied to experimentally determine which membrane composition optimizes the linear response range.

ASSOCIATED CONTENT

Supporting Information

The Supporting Information is available free of charge at ….

Further experimental details, including the synthesis and characterization of ETH500-m. Mathematical procedures to solve the set of Equations 2 to 6. Calculation of the concentration of ISE membrane species. Calculation of hydrogen phthalate concentration in aqueous samples as a function of pH. Quantitative prediction of the effect of membrane-internal diffusion potentials on potentiometric responses.

AUTHOR INFORMATION

Corresponding Author

Philippe Bühlmann – *Department of Chemistry, University of Minnesota, Minneapolis, Minnesota 55455, United States; orcid.org/0000-0001-9302-4674;* Email: buhlmann@umn.edu

Authors

Madeline L. Honig – *Department of Chemistry, University of Minnesota, Minneapolis, Minnesota 55455, United States; orcid.org/0009-0005-6865-4275.*

Ariki Haba – *Department of Chemistry, University of Minnesota, Minneapolis, Minnesota 55455, United States.*

Katie M. F. O'Leary – *Department of Chemistry, University of Minnesota, Minneapolis, Minnesota 55455, United States; orcid.org/0009-0003-8028-0718.*

Emily E. A. Robinson – *Department of Chemistry, University of Minnesota, Minneapolis, Minnesota 55455, United States; orcid.org/*0009-0007-1148-3633

Kuzivakwashe V. Madungwe – *Department of Chemistry, University of Minnesota, Minneapolis, Minnesota 55455, United States; orcid.org/0000-0002-3095-2462.*

Ye Lin – *Emerson Automation Solutions, Shakopee, MN 55379, United States.*

Chad McGuire – *Emerson Automation Solutions, Shakopee, MN 55379, United States.*

ACKNOWLEDGMENTS

Portions of this study were supported by National Science Foundation grant CHE-2203752 and Emerson Automation Solutions, Shakopee, MN, USA. K. M. F. O. acknowledges a National Science Foundation (NSF) REU summer fellowship (Grant CHE-1851990).

REFERENCES

1. Bakker, E.; Pretsch, E., Modern Potentiometry. *Angew. Chem. Int. Ed.* **2007,** *46*, 5660-5668.
2. Ding, J. W.; Qin, W., Recent Advances in Potentiometric Biosensors. *TrAC, Trends Anal. Chem.* **2020,** *124*, 115803.

3. Parrilla, M.; Cuartero, M.; Crespo, G. A., Wearable Potentiometric Ion Sensors. *TrAC, Trends Anal. Chem.* **2019,** *110*, 303-320.
4. Bühlmann, P.; Chen, L. D., Ion-Selective Electrodes With Ionophore-Doped Sensing Membranes. In *Supramolecular Chemistry: From Molecules to Nanomaterials*, Steed, J. W.; Gale, P. A., Eds. Wiley: Chichester, UK, 2012; pp 2539–2580.
5. Bakker, E.; Bühlmann, P.; Pretsch, E., Carrier-Based Ion-Selective Electrodes and Bulk Optodes. 1. General Characteristics. *Chem. Rev.* **1997,** *97*, 3083-3132.
6. Lentner, C., *Geigy Scientific Tables, Vol. 3: Physical Chemistry Composition of Blood, Hematology Somatometric Data, 8th Ed.* Ciba-Geigy: Basel, 1984.
7. Ghoneim, M. T.; Nguyen, A.; Dereje, N.; Huang, J.; Moore, G. C.; Murzynowski, P. J.; Dagdeviren, C., Recent Progress in Electrochemical pH-Sensing Materials and Configurations for Biomedical Applications. *Chem. Rev.* **2019,** *119*, 5248-5297.
8. Manjakkal, L.; Dervin, S.; Dahiya, R., Flexible Potentiometric pH Sensors for Wearable Systems. *RSC Adv.* **2020,** *10*, 8594-8617.
9. Bakker, E.; Xu, A. P.; Pretsch, E., Optimum Composition of Neutral Carrier Based pH Electrodes. *Anal. Chim. Acta* **1994,** *295*, 253-262.
10. Sokalski, T.; Ceresa, A.; Zwickl, T.; Pretsch, E., Large Improvement of the Lower Detection Limit of Ion-Selective Polymer Membrane Electrodes. *J. Am. Chem. Soc.* **1997,** *119*, 11347.
11. Morf, W. E.; Kahr, G.; Simon, W., Reduction of Anion Interference in Neutral Carrrier Liquid-Membrane Electrodes Responsive to Cations. *Anal. Lett.* **1974,** *7*, 9-22.
12. Buck, R. P.; Tóth, K.; Gràf, E.; Horvai, G.; Pungor, E., Donnan Exclusion Failure in Low Anion Site Density Membranes Containing Valinomycin. *J. Electroanal. Chem.* **1987,** *223*, 51.
13. Bühlmann, P.; Amemiya, S.; Yajima, S.; Umezawa, Y., Co-Ion Interference for Ion Selective Electrodes Based on Charged and Neutral Ionophores: A Comparison. *Anal. Chem.* **1998,** *70*, 4291-4303.
14. Bakker, E.; Bühlmann, P.; Pretsch, E., The Phase-Boundary Potential Model. *Talanta* **2004,** *63*, 3-20.
15. Ogawara, S.; Carey, J. L.; Zou, X. U.; Bühlmann, P., Donnan Failure of Ion-Selective Electrodes with Hydrophilic High-Capacity Ion-Exchanger Membranes. *ACS Sens.* **2016,** *1*, 95-101.
16. Bobacka, J., Conducting Polymer-Based Solid-State Ion-Selective Electrodes. *Electroanalysis* **2006,** *18*, 7-18.
17. Michalska, A., All-Solid-State Ion Selective and All-Solid-State Reference Electrodes. *Electroanalysis* **2012,** *24*, 1253-1265.
18. Hu, J. B.; Stein, A.; Bühlmann, P., Rational Design of All-Solid-State Ion-Selective Electrodes and Reference Electrodes. *TrAC Trends Anal. Chem.* **2016,** *76*, 102-114.
19. Rousseau, C. R.; Bühlmann, P., Calibration-Free Potentiometric Sensing With Solid-Contact Ion-Selective Electrodes. *TrAC Trends Anal. Chem.* **2021,** *140*, 116277.
20. Lindner, E.; Gyurcsányi, R. E., Quality Control Criteria for Solid-Contact, Solvent Polymeric Membrane Ion-Selective Electrodes. *J. Solid State Electrochem.* **2009,** *13*, 51-68.
21. Schulthess, P.; Shijo, Y.; Pham, H. V.; Pretsch, E.; Ammann, D.; Simon, W., A Hydrogen Ion-Selective Liquid-Membrane Electrode Based on Tri-*n*-dodecylamine as Neutral Carrier. *Anal. Chim. Acta* **1981,** *131*, 111-116.
22. Ammann, D.; Lanter, F.; Steiner, R. A.; Schulthess, P.; Shijo, Y.; Simon, W., Neutral Carrier Based Hydrogen-Ion Selective Microelectrode for Extracellular and Intracellular Studies. *Anal. Chem.* **1981,** *53*, 2267-2269.

23. Chao, P.; Ammann, D.; Oesch, U.; Simon, W.; Lang, F., Extracellular and Intracellular Hydrogen Ion-Selective Microelectrode Based on Neutral Carriers With Extended pH Response Range in Acid Media. *Pfluegers Arch. Eur. J. Physiol.* **1988,** *411*, 216-219.
24. Yuan, R.; Wu, H. L.; Yu, R. Q., Membrane pH-Sensitive Electrodes Base on New Nitrogen-Containing Neutral Carriers. *Sci. China, Ser. B: Chem.* **1993,** *36*, 140-150.
25. Yuan, R.; Chai, Y. Q.; Yu, R. Q., Poly(vinyl chloride) Matrix Membrane pH Electrode Based on 4,4'-Bis(*N,N*-Dialkylamino)methylazobenzene With a Wide Linear pH Response Range. *Analyst* **1992,** *117*, 1891-1898.
26. Egorov, V. V.; Siamionau, A. V.; Ragoyja, E. G., H^+-Selective Electrodes Based on Amine-Type Ionophores: Generalized Theory and A Priori Quantification of Lower and Upper Detection Limits. *ACS Sens.* **2023,** *8*, 2087-2095.
27. Boswell, P. G.; Szijjarto, C.; Jurisch, M.; Gladysz, J. A.; Rabai, J.; Buhimann, P., Fluorophilic Ionophores for Potentiometric pH Determinations with Fluorous Membranes of Exceptional Selectivity. *Anal. Chem.* **2008,** *80*, 2084-2090.
28. Boswell, P. G.; Sziíjártó, C.; Jurisch, M.; Gladysz, J. A.; Rábai, J.; Bühlmann, P., Fluorophilic Ionophores for Potentiometric pH Determinations with Fluorous Membranes of Exceptional Selectivity (vol 80, pg 2084, 2008). *Anal. Chem.* **2020,** *92*, 16338-16338.
29. Chen, X. V.; Mousavi, M. P. S.; Bühlmann, P., Fluorous-Phase Ion-Selective pH Electrodes: Electrode Body and Ionophore Optimization for Measurements in the Physiological pH Range. *ACS Omega* **2020,** *5*, 13621-13629.
30. Choi, K. R.; Honig, M. L.; Bühlmann, P., Covalently Attached Ionophores to Extend the Working Range of Potentiometric pH Sensors with Poly(decyl methacrylate) Sensing Membranes. *Analyst* **2024**, *149*, 1132–1140.
31. Choi, K. R.; Chemical and Physical Limitations of Electrochemical Sensors, PhD thesis, University of Minnesota, Minneapolis, 2024.
32. Youden, W. J.; Dobroscky, I. D., A Capillary Glass Electrode. *Contrib. Boyce Thompson Inst.* **1931,** *3*, 347-62.
33. MacInnes, D. A.; Belcher, D.; Shedlovsky, T., The Meaning and Standardization of the pH Scale. *J. Am. Chem. Soc.* **1938,** *60*, 1094-1099.
34. Manov, G. G.; Delollis, N. J.; Acree, S. F., Comparative Liquid-Junction Potentials of Some pH Buffer Standards and the Calibration of pH Meters. *J. Res. Natl. Bur. Stand. (U. S.)* **1945,** *34*, 115-127.
35. Rousseau, C. R.; Chipangura, Y. E.; Stein, A.; Bühlmann, P., Effect of Ion Identity on Capacitance and Ion-to-Electron Transduction in Ion-Selective Electrodes with Nanographite and Carbon Nanotube Solid Contacts. *Langmuir* **2024**, *40*, 3, 1785–1792.
36. Choi, K. R.; Troudt, B. K.; Bühlmann, P., Ion-Selective Electrodes With Sensing Membranes Covalently Attached to Both the Inert Polymer Substrate and Conductive Carbon Contact. *Angew. Chem. Int. Ed.* **2023,** *62*, e20230467.
37. Bakker, E.; Nägele, M.; Schaller, U.; Pretsch, E., Applicability of the Phase Boundary Potential Model to the Mechanistic Understanding of Solvent Polymeric Membrane-Based Ion-Selective Electrodes. *Electroanalysis* **1995,** *7*, 817-822.
38. Amemiya, S.; Bühlmann, P.; Umezawa, Y., A Phase Boundary Potential Model for Apparently "Twice-Nernstian" Responses of Liquid Membrane Ion-Selective Electrodes. *Anal. Chem.* **1998,** *70*, 445-454.
39. Marcus, Y., A Simple Empirical Model Describing the Thermodynamics of Hydration of Ions of Widely Varying Charges, Sizes, and Shapes. *Biophys. Chem.* **1994,** *51*, 111-127.
40. Buck, R. P.; Lindner, E., Recommendations for Nomenclature of Ion-Selective Electrodes (IUPAC Recommendations 1994). *Pure Appl. Chem.* **1994,** *66*, 2527-2536.

41. Negash, N.; Moges, G.; Chandravanshi, B. S., Liquid Membrane Electrode Based on Brilliant Green-Hydrogen Phthalate Ion Pair. *Chem. Anal. (Warsaw, Pol.)* **1997,** *42*, 579-588.
42. Viçoso, C.; Lito, M. J.; Camoes, M. F., Solubility and osmotic coefficient of phthalic acid aqueous solutions from isopiestic measurements. *Anal. Chim. Acta* **2004,** *514*, 131-135.
43. Kakiuchi, T.; Senda, M., The Liquid-Junction Potential at the Contact of 2 Immiscible Electrolyte Solutions in the Abscence of Supporting Electrolytes Reference Electrodes Reversible to Alkylammonium Ions and Tetraphenylborate Ion in Nitrobenzene. *Bull. Chem. Soc. Jpn.* **1987,** *60*, 3099-3107.
44. Mikhelson, K. N.; Lewenstam, A.; Didina, S. E., Contribution of the Diffusion Potential to the Membrane Potential and to the Ion-Selective Electrode Response. *Electroanalysis* **1999,** *11*, 793-798.
45. Henderson, L. J., Blood as a Physicochemical System. *J. Biol. Chem.* **1921,** *46*, 411-419.
46. Maj-Zurawska, M.; Hulanicki, A., Study of Time Changes of Anion Exchanger Electrode Characteristics. *Mikrochim. Acta* **1990,** *I*, 209-216.
47. Lewenstam, A., Non-Equilibrium Potentiometry-The Very Essence. *J. Solid State Electrochem.* **2011,** *15*, 15-22.
48. Sokalski, T.; Maj-Zurawska, M.; Hulanicki, A., Determination of True Selectivity Coefficients of Neutral Carrier Calcium Selective Electrode. *Mikrochim. Acta* **1991,** *I*, 285-291.
49. Bakker, E.; Pretsch, E., The New Wave of Ion-Selective Electrodes. *Anal. Chem.* **2002,** *74*, 420A-426A.
50. Gyurcsanyi, R. E.; Pergel, E.; Nagy, R.; Kapui, I.; Lan, B. T. T.; Toth, K.; Bitter, I.; Lindner, E., Direct Evidence of Ionic Fluxes Across Ion Selective Membranes: A Scanning Electrochemical Microscopic and Potentiometric Study. *Anal. Chem.* **2001,** *73*, 2104-2111.
51. Malon, A.; Vigassy, T.; Bakker, E.; Pretsch, E., Potentiometry at Trace Levels in Confined Samples: Ion-Selective Electrodes with Subfemtomole Detection Limits. *J. Am. Chem. Soc.* **2006,** *128*, 8154-8155.
52. Hernández, T. A.; Mayorga, F.; Garcia, J. I.; Zanotto, F. M.; Fernández, R. A.; Dassie, S. A., Facilitated Ion Transfer Reactions Across Liquid|Liquid Interfaces Assisted by a Neutral Weak Acid: A Theoretical Approach, *ChemElectroChem* **2022**, *9*, e202200415.
53. Materova, E. A.; Grekovich, A. L.; Garbuzova, N. V., Ion-Selective Nitrate Electrode for Acid Media. *J. Anal. Chem.* **1974,** *29*, 1638-1642.
54. Materova, E. A.; Garbuzova, N. V., Ion-Selective Film Electrodes With Membranes on Basis of a Series of Liquid Anion-Exchangers in Nitric Acid Solutions. *Sov. Electrochem.* **1977,** *13*, 1592-1595.
55. Bühlmann, P.; Umezawa, Y., Apparently "Non-Nernstian" Equilibrium Responses Based on Complexation Between the Primary Ion and a Secondary Ion in the Liquid ISE Membrane. *Electroanalysis* **1999,** *11*, 687-693.
56. Amemiya, S.; Bühlmann, P.; Odashima, K., A Generalized Model for Apparently “Non-Nernstian" Equilibrium Responses of Ionophore-Based Ion-Selective Electrodes. 1. Independent Complexation of the Ionophore with Primary and Secondary Ions. *Anal. Chem.* **2003,** *75*, 3329-3339.
57. Koseoglu, S. S.; Lai, C.-Z.; Ferguson, C.; Bühlmann, P., Response Mechanism of Ion-Selective Electrodes Based on a Guanidine Ionophore: An Apparently ‘Two-Thirds Nernstian' Response Slope. *Electroanalysis* **2008,** *20*, 331-339.
58. Miyake, M.; Chen, L. D.; Pozzi, G.; Bühlmann, P., Ion-Selective Electrodes with Unusual Response Functions: Simultaneous Formation of Ionophore-Primary Ion Complexes with Different Stoichiometries. *Anal. Chem.* **2012,** *84*, 1104-1111.

59. Amemiya, S.; Buhlmann, P.; Pretsch, E.; Rusterholz, B.; Umezawa, Y., Cationic or anionic sites? Selectivity optimization of ion-selective electrodes based on charged ionophores. *Anal. Chem.* **2000,** *72*, 1618-1631.

TOC image